

# Numerically exact and approximate determination of energy eigenvalues for antiferromagnetic molecules using irreducible tensor operators and general point-group symmetries

Roman Schnalle\*

*Fachbereich Physik, Universität Osnabrück, D-49069 Osnabrück, Germany*

Jürgen Schnack†

*Fakultät für Physik, Universität Bielefeld, Postfach 100131, D-33501 Bielefeld, Germany*

(Received 22 December 2008; revised manuscript received 12 February 2009; published 19 March 2009)

For small-enough quantum systems numerical exact and complete diagonalization of the Hamiltonian enables one to evaluate and discuss all static, dynamic, and thermodynamic properties. In this article we consider Heisenberg spin systems and extend the range of applicability of the exact diagonalization method by showing how the irreducible tensor operator technique can be combined with an unrestricted use of general point-group symmetries. We also present ideas on how to use spin-rotational and point-group symmetries in order to obtain approximate spectra.

DOI: [10.1103/PhysRevB.79.104419](https://doi.org/10.1103/PhysRevB.79.104419)

PACS number(s): 75.10.Jm, 75.50.Xx, 75.40.Mg, 75.50.Ee

## I. INTRODUCTION

The knowledge of energy spectra of small magnetic systems such as magnetic molecules is indispensable for the (complete) understanding of their spectroscopic, dynamic, and thermodynamic properties. In this respect numerical exact diagonalization of the appropriate quantum Hamiltonian is a highly desired method. Nevertheless, such an attempt is very often severely restricted due to the huge dimension of the underlying Hilbert space. For a magnetic system of  $N$  spins of spin quantum number  $s$  the dimension is  $(2s+1)^N$  which grows exponentially with  $N$ . Group theoretical methods can help to ease this numerical problem. A further benefit is given by the characterization of the obtained energy levels by quantum numbers and classification according to irreducible representations.

Along these lines much effort has been put into the development of an efficient numerical diagonalization technique of the Heisenberg model using irreducible tensor operators, i.e., employing the full rotational symmetry of angular momenta.<sup>1-6</sup> A combination of this meanwhile well-established technique with point-group symmetries is not very common since a rearrangement of spins due to point-group operations easily leads to complicated basis transformations between different coupling schemes. A possible compromise is to use only part of the spin-rotational symmetry (namely, rotations about the  $z$  axis) together with point-group symmetries<sup>7</sup> or to expand all basis states in terms of simpler product states.<sup>8-10</sup> To the best of our knowledge only few attempts have been undertaken to combine the full spin-rotational symmetry with point-group symmetries. Waldmann<sup>11</sup> combined the full spin-rotational symmetry with those point-group symmetries that are compatible with the spin coupling scheme, i.e., avoid complicated basis transforms between different coupling schemes. Especially low-symmetry groups such as  $D_2$  are often applicable since the coupling scheme can be organized accordingly; compare Ref. 12 for an early investigation. Bostrem *et al.*<sup>13</sup> and

Sinitsyn *et al.*<sup>14</sup> followed a similar route for the square lattice antiferromagnet by employing  $D_4$  point-group symmetry. This already establishes a very powerful numerical method.

In this article we show how the irreducible tensor operator technique can be combined with an unrestricted use of general point-group symmetries. The problem, that the application of point-group operations leads to states belonging to a basis characterized by a different coupling scheme whose representation in the original basis is not (easily) known, can be solved by means of graph theoretical methods that have been developed in another context.<sup>15,16</sup> We discuss how these methods can be implemented and present results for numerical exact diagonalizations of Heisenberg spin systems of unprecedented size.

Having these methods developed we also discuss ideas of approximately obtaining energy spectra of so-called bipartite, i.e., nonfrustrated, antiferromagnetic spin systems. The idea is to perform numerical diagonalizations in the orthogonal Hilbert subspaces characterized by spin and point-group quantum numbers using only a restricted but carefully chosen basis subset. We demonstrate how this idea works for archetypical spin systems such as bipartite or slightly frustrated spin rings. The advantage compared to alternative approximate methods such as density matrix renormalization group<sup>17-19</sup> (DMRG), Lanczos,<sup>20</sup> or quantum Monte Carlo<sup>21-23</sup> (QMC) techniques is that one obtains many energy levels together with their spectroscopic classification which can be of great use for the discussion of electron paramagnetic resonance (EPR), nuclear magnetic resonance (NMR), or inelastic neutron scattering (INS) spectra. In this respect our idea can provide a valuable complement to the already established approximate methods.

The article is organized as follows. In Sec. II we explain the idea of a combined usage of spin-rotational and point-group symmetries. Section III provides examples for full diagonalization studies. Our approximate diagonalization scheme is introduced in Sec. IV, whereas Sec. V provides example calculations on bipartite systems. The paper closes with a summary.

## II. THEORETICAL METHOD

### A. Irreducible tensor operator approach

The physics of many magnetic molecules can be well understood with the help of the isotropic Heisenberg model with nearest-neighbor coupling. The action of an external magnetic field is accounted for by an additional Zeeman term. The resulting Hamiltonian then looks like

$$\underline{H} = - \sum_{i,j} J_{ij} \underline{\mathfrak{s}}(i) \cdot \underline{\mathfrak{s}}(j) + g \mu_B \underline{\mathfrak{S}} \cdot \vec{B}. \quad (1)$$

The sum reflects the exchange interaction between single spins given by spin operators  $\underline{\mathfrak{s}}$  at sites  $i$  and  $j$ . For the sake of simplicity we assume a common isotropic  $g$  tensor. Then the Zeeman term couples the total-spin operator  $\underline{\mathfrak{S}} = \sum_{i=1}^N \underline{\mathfrak{s}}(i)$  to the external magnetic field  $\vec{B}$ . A negative value of  $J_{ij}$  refers to an antiferromagnetic coupling.

For the following discussion an antiferromagnetic nearest-neighbor exchange coupling of constant value  $J < 0$  is assumed (which can easily be generalized), then the Heisenberg part can be written as

$$\underline{H}_{\text{Heisenberg}} = -J \sum_{\langle i,j \rangle} \underline{\mathfrak{s}}(i) \cdot \underline{\mathfrak{s}}(j), \quad (2)$$

where the summation parameter  $\langle i,j \rangle$  indicates the summation running over nearest-neighbor spins counting each pair only once. Since the commutation relations,

$$[\underline{H}_{\text{Heisenberg}}, \underline{\mathfrak{S}}] = 0, \quad (3)$$

hold it is possible to find a common eigenbasis  $\{|\nu\rangle\}$  of  $\underline{H}_{\text{Heisenberg}}$ ,  $\underline{\mathfrak{S}}^2$ , and  $\underline{\mathfrak{S}}_z$ . We denote the corresponding eigenvalues as  $E_\nu$ ,  $S_\nu$ , and  $M_\nu$ . Due to spin-rotational symmetry [Eq. (3)], the eigenvalues of Hamiltonian (1) can be evaluated (later) according to

$$E_\nu(B) = E_\nu + g \mu_B B M_\nu, \quad (4)$$

where the direction of the external field  $\vec{B}$  defines the  $z$  axis.

Calculating the eigenvalues here corresponds to finding a matrix representation of the Hamiltonian and diagonalizing it numerically. A very efficient and elegant way of finding the matrix elements of Eq. (2) is based on the use of irreducible tensor operators. Apart from its elegance it drastically reduces the dimensionality of the problem because it becomes possible to work directly within the subspace  $\mathcal{H}(S, M=S)$  of the total Hilbert space  $\mathcal{H}$  characterized by quantum numbers  $S$  and  $M=S$ ; for typical dimensions compare, for instance, Ref. 24.

The calculation of matrix elements of the given Hamiltonian using irreducible tensor operators is compulsorily related to the application of the Wigner-Eckart theorem. The Wigner-Eckart theorem

$$\begin{aligned} \langle \alpha S M | \underline{T}_q^{(k)} | \alpha' S' M' \rangle &= (-1)^{S-M} \langle \alpha S | \underline{\mathbb{T}}^{(k)} | \alpha' S' \rangle \\ &\times \begin{pmatrix} S & k & S' \\ -M & q & M' \end{pmatrix} \end{aligned} \quad (5)$$

states that a matrix element of the  $q$ th component of an irreducible tensor operator  $\underline{\mathbb{T}}^{(k)}$  of rank  $k$  is given by the reduced

matrix element  $\langle \alpha S | \underline{\mathbb{T}}^{(k)} | \alpha' S' \rangle$  and a factor containing a Wigner-3J symbol.<sup>25</sup>

It should be emphasized that the reduced matrix element is completely independent of any magnetic quantum number  $M$ . The basis in Eq. (5) is given following the well-known vector-coupling scheme. The quantum number  $\alpha$  within the ket  $|\alpha S M\rangle$  refers to a set of intermediate spin quantum numbers resulting from the coupling of single spins  $s$  to the total-spin quantum number  $S$ . In order to apply the Wigner-Eckart theorem it is necessary to express the Heisenberg Hamiltonian in Eq. (2) with the help of irreducible tensor operators. Therefore the single-spin vector operators  $\underline{\mathfrak{s}}(i)$  can be seen as irreducible tensor operators of rank  $k=1$  with components  $q=-1, 0, 1$ . The relation to the components of the vector operators is given by

$$\underline{\mathfrak{s}}_0^{(1)} = \underline{\mathfrak{s}}^z, \underline{\mathfrak{s}}_{\pm 1}^{(1)} = \mp \sqrt{\frac{1}{2}} (\underline{\mathfrak{s}}^x \pm i \underline{\mathfrak{s}}^y). \quad (6)$$

Writing the Heisenberg exchange term as a tensor product of the single-spin irreducible tensor operators results in<sup>2</sup>

$$\underline{H}_{\text{Heisenberg}} = \sqrt{3} J \sum_{\langle i,j \rangle} \underline{T}^{(0)}(\{k_l\}, \{\bar{k}_m\} | k_i = k_j = 1). \quad (7)$$

$\underline{T}^{(0)}$  is a zero-rank irreducible tensor operator depending on the set  $\{k_l\}$ ,  $l=1, \dots, N$ , which gives the ranks of single-spin irreducible tensor operators and  $\{\bar{k}_m\}$ ,  $m=1, \dots, N-1$ , which refers to the ranks of intermediate irreducible tensor operators. In a successive coupling scheme within a system of  $N$  spins an irreducible tensor operator of this kind would look like

$$\begin{aligned} \underline{T}^{(0)}(\{k_l\}, \{\bar{k}_m\}) &= \{ \dots \{ [\underline{\mathfrak{s}}^{(k_1)}(1) \otimes \underline{\mathfrak{s}}^{(k_2)}(2)]^{\bar{k}_1} \otimes \underline{\mathfrak{s}}^{(k_3)} \\ &\times (3) \}^{\bar{k}_2} \dots \}^{\bar{k}_{N-2}} \otimes \underline{\mathfrak{s}}^{(k_N)}(N)^{(0)}. \end{aligned} \quad (8)$$

The notation  $\underline{T}^{(0)}(\{k_l\}, \{\bar{k}_m\} | k_i = k_j = 1)$  corresponds to the situation in which the ranks of all single-spin tensor operators are zero except those at sites  $i$  and  $j$  which are tensor operators of rank 1.

The set  $\{\bar{k}_m\}$  results from the chosen coupling scheme, for example, of the form of Eq. (8), with known ranks of single-spin tensor operators taking into account addition rules for spin quantum numbers of the vector-coupling scheme such as  $\bar{k}_1 = |k_1 - k_2|, \dots, k_1 + k_2$ .

After writing the Heisenberg Hamiltonian as a sum of irreducible tensor operators, the matrix elements within a basis of the form  $|\alpha S M\rangle$  can be calculated by the application of the Wigner-Eckart theorem. The reduced matrix elements are determined using the so-called *decoupling* procedure.<sup>3,4</sup> Since the irreducible tensor operator  $\underline{\mathbb{T}}^{(k)}$  is given as a tensor product of irreducible tensor operators with regard to a certain coupling scheme [comp. Eq. (8)], the reduced matrix element  $\langle \alpha S | \underline{\mathbb{T}}^{(k)} | \alpha' S' \rangle$  can successively be decomposed into a product of single-spin irreducible tensor operators and Wigner-9J symbols.

### B. General point-group symmetries

The use of irreducible tensor operators for the calculation of the matrix elements of the Hamiltonian and as a result also of the energy spectrum is essential for the treatment of magnetic molecules containing many interacting paramagnetic ions. Nevertheless, it is sometimes necessary to further reduce the dimensionality of the problem, either because computational resources are limited or a labeling of certain energy levels becomes advantageous, e.g., for spectroscopic classification.<sup>26,27</sup> Such a reduction can be done if the Hamiltonian remains invariant under certain permutations of spin centers. Often the spin-permutational symmetry of the Hamiltonian coincides with spatial symmetries of the molecule, i.e., point-group symmetries; therefore the term point-group symmetry is used while one refers to the invariance of the Hamiltonian under permutations of spins.

Using point-group symmetries of the system results in a decomposition of the Hamilton matrix  $\langle \alpha SM | \underline{H} | \alpha' SM \rangle$  into irreducible representations  $\Gamma^{(n)}(\mathcal{G})$  of a group  $\mathcal{G}$  whose elements  $\mathcal{G}(R)$ , i.e., the operators corresponding to the symmetry operations  $R$ , do commute with  $\underline{H}$ . The symmetrized basis functions that span the irreducible representations  $n$  are found by the application of the projection operator  $\mathcal{P}^{(n)}$  to the full set of basis vectors  $|\alpha SM\rangle$  and subsequent orthonormalization. The overcomplete set of basis states  $\{|\alpha SM \Gamma^{(n)}\rangle\}$  spanning the  $n$ th irreducible representation  $\Gamma^{(n)}(\mathcal{G})$  is generated by<sup>28</sup>

$$\mathcal{P}^{(n)}|\alpha SM\rangle = \left\{ \frac{l_n}{h} \sum_R [\chi^{(n)}(R)]^* \mathcal{G}(R) \right\} |\alpha SM\rangle, \quad (9)$$

where  $l_n$  is the dimension of the irreducible representation  $\Gamma^{(n)}$ ,  $h$  denotes the order of  $\mathcal{G}$ , and  $\chi^{(n)}(R)$  is the character of the  $n$ th irreducible representation of the symmetry operation  $R$ .

Equation (9) contains the main challenge while creating symmetrized basis states. The action of the operators  $\mathcal{G}(R)$  on basis states of the form  $|\alpha SM\rangle$  has to be known. Of course, one could expand  $|\alpha SM\rangle$  into a linear combination of product states  $|m_1 m_2 \dots m_N\rangle$ . Then the action of  $\mathcal{G}(R)$  leads to a permutation of magnetic quantum numbers  $m_i$  within the ket  $|m_1 m_2 \dots m_N\rangle$ . But, the recombination of the symmetry-transformed product states into basis states  $|\alpha SM\rangle$  will then be much too time consuming for larger systems.

Following Ref. 11 the action of  $\mathcal{G}(R)$  on states  $|\alpha SM\rangle$  can directly be evaluated without expanding it into product states. Suppose there is a certain coupling scheme  $a$  in which spin operators  $\mathfrak{s}(i)$  are coupled to yield the total-spin operator  $\mathfrak{S}$ . Generally the action of operators  $\mathcal{G}(R)$  on states  $|\alpha SM\rangle$  leads to a different coupling scheme  $b$ . Now those states which belong to the coupling scheme  $b$  have to be reconverted into a linear combination of states belonging to  $a$ . This is technically a rather involved calculation, and one would not like to do it by hand and for every coupling scheme separately. To the best of our knowledge it has never been noted or even used that the conversion from any arbitrary (!) coupling scheme  $b$  into the desired coupling scheme  $a$  can be well automatized. Suppose there is a state  $|\alpha SM\rangle_a$  belonging to the coupling scheme  $a$ . The action of an arbitrary

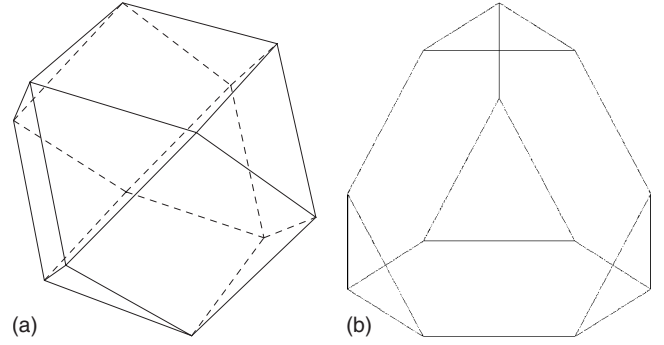


FIG. 1. Structure of the cuboctahedron (l.h.s.) and the truncated tetrahedron (r.h.s.) (Ref. 29).

group element  $\mathcal{G}(R)$  results in a state  $|\alpha SM\rangle_b$  belonging to a different coupling scheme  $b$ . Then the re-expression takes the following form:

$$\mathcal{G}(R)|\alpha SM\rangle_a = \sum_{\alpha'} |\alpha' SM\rangle_a \langle \alpha' SM | \alpha SM \rangle_b, \quad (10)$$

where a term like  $\langle \alpha' SM | \beta SM \rangle_b$  is known as *general recoupling coefficient*. The calculation of general recoupling coefficients and the evaluation of Eq. (10) can be performed with the help of graph theoretical methods.<sup>15,16</sup>

An implementation of these methods within a computer program is a straightforward task (follow directions given in Refs. 15 and 16). Nevertheless, we would like to provide some practical comments. Since such a program should be as general as possible, it does not employ analytical solutions (as done for the  $D_4$  symmetry in Refs. 13 and 14) but numerical solutions. This concerns the reorthogonalization of the overcomplete set of basis states  $\{|\alpha SM \Gamma^{(n)}\rangle\}$  spanning the  $n$ th irreducible representation  $\Gamma^{(n)}(\mathcal{G})$ , which is performed with a Gram-Schmidt orthogonalization procedure, as well as the evaluation of the generalized recoupling coefficients which is numerically done as described in Refs. 15 and 16. A considerable computational speedup can be achieved by tabulating Wigner-9J symbols beforehand since they are heavily used during the calculations.

### III. NUMERICAL EXACT DIAGONALIZATION

In this section we would like to present two applications for realistic spin systems that can be treated using irreducible tensor operator techniques and point-group symmetries, but not otherwise. Both systems—cuboctahedron and truncated tetrahedron—consist of  $N=12$  spins of spin quantum number  $s=3/2$  (Hilbert space dimension 16 777 216). The two spin systems, which are realized as antiferromagnetic molecules—cuboctahedron<sup>30</sup> and truncated tetrahedron<sup>31</sup> (see Fig. 1 for the structure)—belong to the class of geometrically frustrated spin systems<sup>32–34</sup> and are thus hardly accessible by means of quantum Monte Carlo.

Figure 2 shows the energy spectrum of the antiferromagnetic cuboctahedron with  $s=3/2$ . This spectrum was obtained using only  $D_2$  point-group symmetry which is already sufficient in order to obtain sufficiently small Hamilton matrices. In addition Fig. 3 demonstrates for the subspaces of

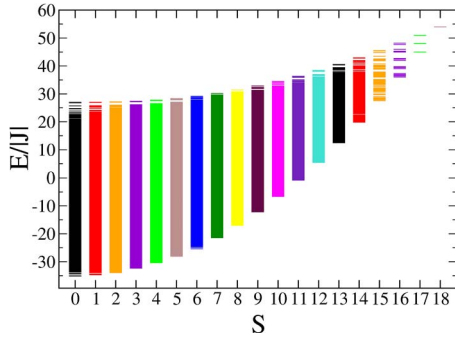


FIG. 2. (Color online) Complete energy spectrum of the antiferromagnetic cuboctahedron with  $s=3/2$ .

total spin  $S=0$  and  $S=1$  that a representation in the full  $O_h$  group can be achieved which yields level assignments according to the irreducible representations of this group.

A complete energy spectrum allows to calculate thermodynamic properties as functions of both temperature  $T$  and magnetic field  $B$ . For the cuboctahedron this was already done elsewhere.<sup>34</sup> Therefore, we would like to discuss another frustrated structure: the truncated tetrahedron which was synthesized quite recently.<sup>31</sup> In principle this geometry permits two different exchange constants: one inside the triangles ( $J_1$ ) and the other between the triangles ( $J_2$ ) (compare Fig. 1). A practical symmetry for this molecule is, for instance,  $C_{2v}$ , whereas the full symmetry is  $T_d$ . Figure 4 displays the complete energy spectrum for the case  $J_1=J_2=J$ . The inset of Fig. 4 magnifies the low-energy sector. As in the case of many other frustrated antiferromagnetic systems the spectrum exhibits more than one singlet below the first triplet.<sup>32</sup>

In Fig. 5 we show the zero-field specific heat (top) as well as the zero-field differential magnetic susceptibility (bottom). The fine structure of the specific heat, which is especially pronounced for  $s=3/2$ , results from the low-energy gap structure. The sharp peak is an outcome of the gap between the lowest singlet and the group of levels around the second singlet and the first two triplets, the latter being highly degenerate (both ninefold including  $M$  degeneracy). This unusual degeneracy of the lowest triplets is also the origin of the quick rise and subsequent flat behavior of the susceptibility in the case of  $s=3/2$ .

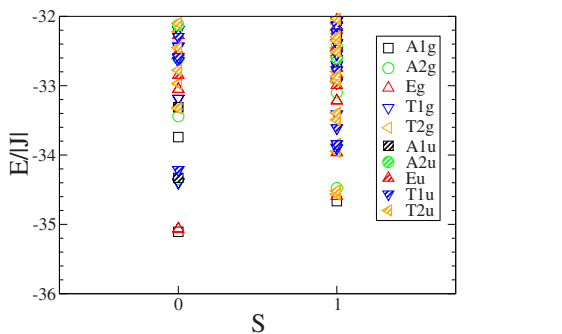


FIG. 3. (Color online) Low-lying energy spectrum of the antiferromagnetic cuboctahedron with  $s=3/2$  in subspaces of  $S=0$  and  $S=1$ . The symbols denote the irreducible representations of the  $O_h$  group.

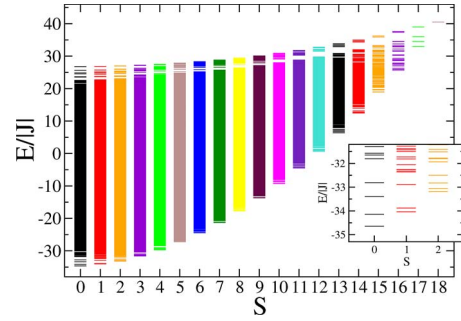


FIG. 4. (Color online) Complete energy spectrum of the antiferromagnetic truncated tetrahedron with  $J_1=J_2=J$ . The inset shows low-lying levels in subspaces with  $S=0, 1, 2$ .

In connection with the truncated tetrahedron it might be interesting to realize the technical progress. The truncated tetrahedron with  $s=1/2$  was investigated in 1992.<sup>35</sup> The dimension of its Hilbert space is 4096, whereas the dimension for  $s=3/2$  is 16 777 216.

#### IV. APPROXIMATE DIAGONALIZATION

Sections I–III demonstrate that numerical exact diagonalization in connection with irreducible tensor operators is a powerful tool to investigate thermodynamical properties of large magnetic molecules. Nevertheless, sometimes the use of total-spin and point-group symmetries is not sufficient to obtain small-enough matrices. For such cases we suggest an approximate diagonalization in this section. The approximation is partially based on perturbation theory arguments. First ideas along this line were already suggested in Ref. 36. We will generalize and largely extend this idea.

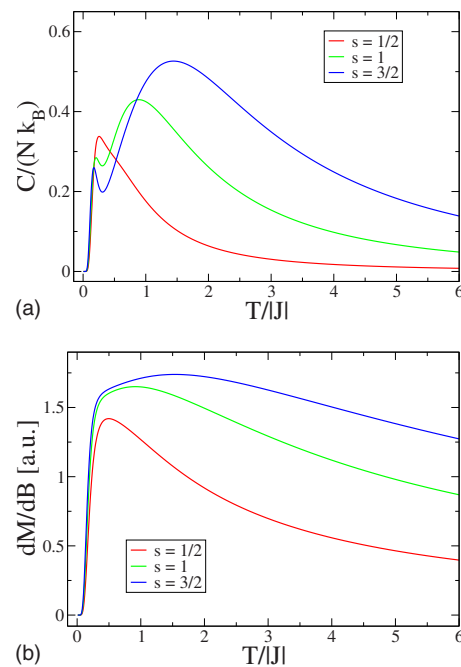


FIG. 5. (Color online) Specific heat  $c(T, B=0)$  (top) and differential magnetic susceptibility  $\chi(T, B=0)$  (bottom) of the truncated tetrahedron with  $J_1=J_2=J$ .

Let us assume that the spin system is described by a Hamiltonian  $\underline{H}$  which acts in the Hilbert space  $\mathcal{H}$ . Suppose there is a zeroth-order Hamiltonian  $\underline{H}_0$  and a decomposition according to

$$\underline{H} = \underline{H}_0 + \lambda \underline{H}' . \quad (11)$$

In the case of nondegenerate eigenstates  $|\phi_i^{(0)}\rangle$  of  $\underline{H}_0$  the series expansion,

$$|\phi_i\rangle = |\phi_i^{(0)}\rangle + \lambda |\phi_i^{(1)}\rangle + \lambda^2 |\phi_i^{(2)}\rangle + \dots , \quad (12)$$

$$E_i = E_i^{(0)} + \lambda E_i^{(1)} + \lambda^2 E_i^{(2)} + \dots , \quad (13)$$

holds for the exact eigenstates  $|\phi_i\rangle$  and corresponding eigenvalues  $E_i$ . The index  $i=1, \dots, n$  denotes the states of the system. The energy eigenvalues and eigenstates in zeroth-order result from a (typically simple or even analytical) diagonalization of  $\underline{H}_0$  within an arbitrary basis of  $\mathcal{H}$ .

We label the eigenvalues  $E_i^{(0)}$  and eigenstates  $|\phi_i^{(0)}\rangle$  in such a manner that

$$E_i^{(0)} < E_{i+1}^{(0)}, \quad \forall i = 1, \dots, n-1 \quad (14)$$

holds. Now we do not follow conventional perturbation theory as it would lead to a successive introduction of additional terms within the series expansion in Eq. (12), i.e., terms with increasing order of  $\lambda$ . Instead, we diagonalize the full Hamiltonian  $\underline{H}$  within a reduced set  $\{|\phi_i^{(0)}\rangle\}$ ,  $i = 1, \dots, n_{\text{red}}$ , of eigenstates of  $\underline{H}_0$ , where  $n_{\text{red}} \leq n$  is referred to as *cut-off parameter*. The resulting eigenvalues and eigenstates of this approximation are denoted as  $E_i^{\text{approx}}$  and  $|\phi_i^{\text{approx}}\rangle$ . Such an approximate scheme is always converging since for  $n_{\text{red}}=n=\dim(\mathcal{H})$  all basis states are incorporated and the diagonalization corresponds to an exact treatment of the system; i. e.,

$$E_i^{\text{approx}} \xrightarrow{n_{\text{red}} \rightarrow n} E_i, \quad |\phi_i^{\text{approx}}\rangle \xrightarrow{n_{\text{red}} \rightarrow n} |\phi_i\rangle \quad \forall i. \quad (15)$$

It is clear that the speed of convergence depends on the choice of  $\underline{H}_0$ .

The speed of convergence will be different for the various states. Since the approximate diagonalization is performed with the  $n_{\text{red}}$  low-lying states of  $\underline{H}_0$  according to Eq. (14), one expects that the low-lying energy levels converge quickest against their true values. As in perturbation theory this assumption relies on the hypothesis that energetically higher-lying levels do mix into the desired low-lying state with decreasing weight. In perturbation theory this expresses itself in the second-order corrections

$$E_i^{(2)} = \sum_{i \neq j} \frac{|\langle \phi_i^{(0)} | \underline{H}' | \phi_j^{(0)} \rangle|^2}{E_i^{(0)} - E_j^{(0)}}, \quad (16)$$

which decrease with increasing energetic distance  $E_i^{(0)} - E_j^{(0)}$ . In our approximate diagonalization the diagonal

$$\langle \phi_i^{(0)} | \underline{H} | \phi_i^{(0)} \rangle = E_i^{(0)} + \lambda E_i^{(1)}, \quad (17)$$

$$E_i^{(1)} = \langle \phi_i^{(0)} | \underline{H}' | \phi_i^{(0)} \rangle, \quad (18)$$

and off-diagonal terms  $\langle \phi_i^{(0)} | \underline{H}' | \phi_j^{(0)} \rangle$  of perturbation theory appear as diagonal and off-diagonal matrix elements of the

reduced Hamilton matrix. Therefore, the approximate diagonalization includes zeroth- and first-order by definition and all higher orders partially up to the cutoff. The inclusion of eigenstates belonging to degenerate eigenvalues of  $\underline{H}_0$  poses no problem in our scheme. One should only include all eigenstates of a degenerate eigenvalue into the approximate diagonalization; otherwise the convergence is unnecessarily deteriorated.

### A. Approximate diagonalization based on the rotational-band model

As a zeroth-order approximation  $\underline{H}_0$  of isotropic Heisenberg Hamiltonian (2) the rotational-band Hamiltonian<sup>37-39</sup>

$$\underline{H}_0 \equiv \underline{H}_{\text{RB}} = -\frac{DJ}{2N} \left[ \underline{S}^2 - \sum_{n=1}^{N_s} \underline{S}_n^2 \right]. \quad (19)$$

is chosen.<sup>36</sup> This choice rests on the observation that in bipartite antiferromagnetic spin systems the lowest eigenvalues within subspaces of total spin  $S$  follow the *Landé rule*;<sup>40,41</sup> i.e.,

$$E_{\min}(S) - E_0 \propto S(S+1). \quad (20)$$

The prefactor  $-\frac{DJ}{2N}$  in Eq. (19) can be seen as an effective exchange constant which couples the sublattice spins  $\underline{S}_n$  to the total spin  $\underline{S}$  of the system. The value of  $D$ ,

$$D = 2 \cdot \frac{N_b}{N} \cdot \frac{1}{1 - 1/N_s}, \quad (21)$$

is chosen to match the energy of the ferromagnetic state of the system described by an isotropic Heisenberg Hamiltonian.<sup>37</sup>  $N_s$  denotes the number of sublattices which the classical ground state of the system is composed of;  $N_b$  represents the number of bonds of the system. The eigenstates of  $\underline{H}_{\text{RB}}$  are analytically given in the form  $|S_1 \dots S_{N_s} SM\rangle$ , which is an enormous advantage for the following calculations. The corresponding eigenvalues are

$$E_{\text{RB}}(S_1, \dots, S_{N_s}, S) = -\frac{DJ}{2N} \left[ S(S+1) - \sum_{n=1}^{N_s} S_n(S_n+1) \right]. \quad (22)$$

The spectrum of the rotational-band Hamiltonian consists of eigenvalues that form parabolas, so-called rotational bands. In the following a rotational band is defined as a set of eventually energetically degenerate eigenstates  $|S_1 \dots S_{N_s} SM\rangle$  with fixed values of quantum numbers  $S_n$  of the sublattice spins.

Figure 6 shows the spectrum of the rotational-band Hamiltonian for a spin ring of  $N=8$  spins with  $s=5/2$ . The lowest bands refer to a sublattice spin configuration of  $S_1 = S_2 = 4 \cdot 5/2 = 10$ . The next bands result from a deviation of one sublattice spin from its maximum value  $S_{n,\text{max}} = N/N_s \cdot s$ . In such a way the whole spectrum can be constructed following Eq. (22). The eigenstates of the rotational-band Hamiltonian are highly degenerate due to the many possibilities of combining single spins  $\underline{s}_i$  to the sublattice spins  $\underline{S}_n$  and further on sublattice spins  $\underline{S}_n$  to the total spin  $\underline{S}$ .

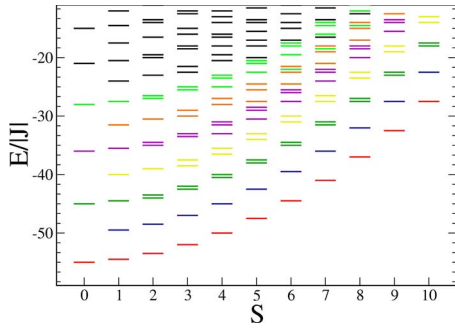


FIG. 6. (Color online) Part of the energy spectra of the rotational-band Hamiltonian for an antiferromagnetic spin ring  $N=8$ , where  $s=5/2$ . Seven superbands are colored.

Figure 6 also shows that the rotational-band spectrum is clustered into *superbands* (highlighted by color). A superband contains those rotational bands for which the sum of sublattice spin quantum numbers is the same. One clearly sees that within the rotational-band spectrum the low-lying superbands are well separated.

Inserting  $H_{RB}$  into Eq. (11) yields

$$H = H_{\text{Heisenberg}} = H_{RB} + H' \quad (23)$$

as a starting point for an approximate diagonalization. With respect to computational resources and due to the fact that the eigenstates of  $H_{RB}$  are given in the form  $|S_1 \dots S_{N_s} SM\rangle$ , the diagonalization is performed in subspaces  $\mathcal{H}(S, M=S)$  using the irreducible tensor operator technique. In addition, point-group symmetries can be used for a further reduction in the dimensionality. However, only those point groups can be applied which do not alter the sublattice structure, i.e., do not lead to rotational bands that are not included in the approximate basis set. Then the symmetry operations on a state belonging to a certain rotational band will always produce states which belong to the same band.

## V. BIPARTITE SYSTEMS—SPIN RING

### A. Convergence

In the following we discuss the properties of the proposed approximate diagonalization for the example of an antiferromagnetic spin ring of  $N=8$  spins with  $s=5/2$ . Figure 7 shows the convergence of the energy levels. In order to label the levels the full symmetry group  $D_8$  of an octagon was used. One clearly sees that the convergence within the  $S=0$  subspace is fast and smooth (looking almost exponential).

In subspaces of  $S=1$  and  $S=2$  the convergence is also fast, but when only few bands are incorporated sharp steps can be observed. This is highlighted by two arrows in the bottom graph of Fig. 7. The stepwise convergence is continued in subspaces with  $S>2$  in a very regular way. It can be observed that with increasing energy within a certain subspace  $\mathcal{H}(S, M=S)$  the steps are slightly washed out. The occurrence of the steps depends on the rotational band the states belong to. For example, the energy of the lowest state (i.e., the first rotational band) within  $\mathcal{H}(S=2, M=2)$  is decreasing if seven bands are incorporated into the approxi-

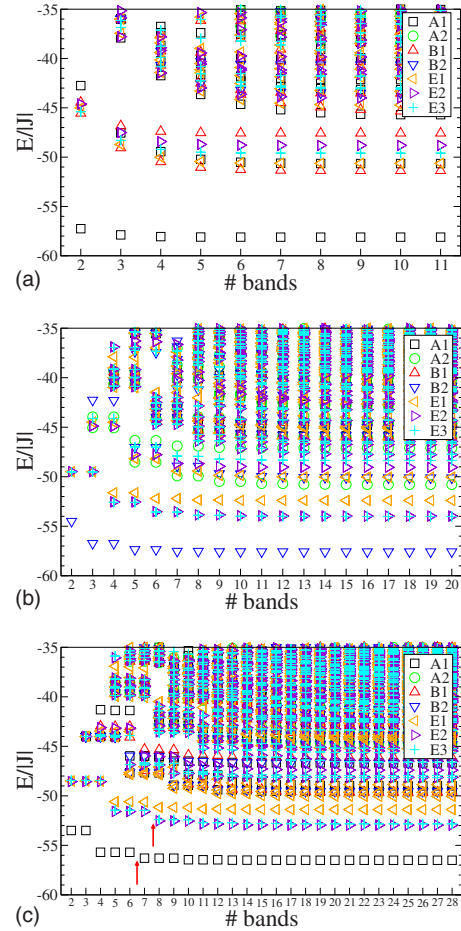


FIG. 7. (Color online) Energy levels of an antiferromagnetic spin ring  $N=8$  with  $s=5/2$  as a function of the number of occupied rotational bands used for diagonalization in subspaces  $S=0$  (top),  $S=1$  (center), and  $S=2$  (bottom). The arrows in the  $S=2$  subspace refer to the steps within the convergence behavior mentioned in the text. The states are labeled according to irreducible representations of  $D_8$ .

mate diagonalization while the energies of states belonging to the second rotational band are lowered if eight bands are incorporated; see also discussion in Sec. V B.

In Fig. 8 the convergence of some low-lying eigenstates of this spin ring is presented. The convergence behaves in analogy to the convergence of the eigenvalues. The stepwise convergence in  $S=1$  becomes obvious. Nevertheless, while using only a fraction of basis states (approximately 30% of the basis states within each subspace) the approximate low-lying eigenstates are practically converged against the exact eigenstates. In addition, it can be seen that states of higher energy converge slower than low-lying states.

We also investigate the convergence for various single-spin quantum numbers  $s$ . In Fig. 9 the relative difference between the approximate energy values and the exact values is displayed for various  $s$  in the subspace  $S=0$ . The levels which have been chosen belong to the first three occupied rotational bands. One clearly sees that the approximate diagonalization converges more rapidly the higher the single spin is. This is not surprising since rotational-band model

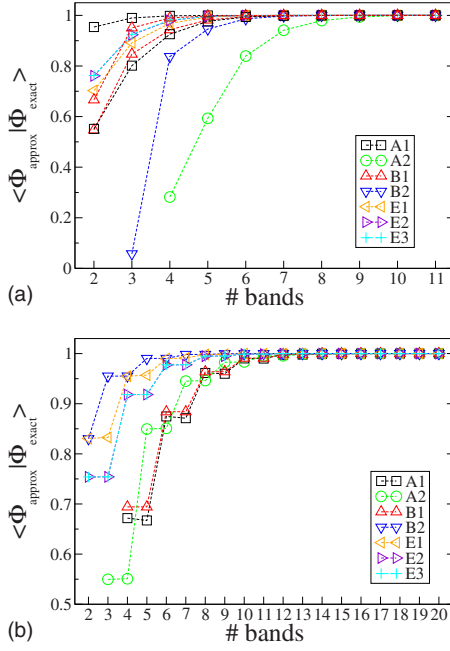


FIG. 8. (Color online) Convergence of the eigenstates of an antiferromagnetic spin ring  $N=8$  with  $s=5/2$  as a function of the number of occupied rotational bands used for diagonalization in subspaces  $S=0$  (top) and  $S=1$  (bottom). The states are labeled according to irreducible representations of  $D_8$ .

(19), which is based on classical assumptions, is itself more accurate the larger  $s$  is.

### B. Approximate selection rule

It turns out that the aforementioned occurrence of steps can be understood and even be employed for a further reduction in the size of Hamilton matrices. The underlying reason is that the full Hamiltonian connects states belonging to different rotational bands with very different strength. After having inspected the reduced Hamilton matrices of various

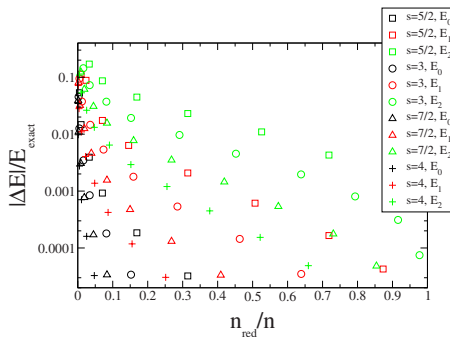


FIG. 9. (Color online) Relative difference between approximate and exact energy eigenvalues for the lowest states of the first three occupied rotational bands for an antiferromagnetic spin ring  $N=8$  with various  $s$  and total spins  $S=0$ .  $E_0$  refers to the energy of the lowest state of the first rotational band,  $E_1$  to the lowest state of the second rotational band and  $E_3$  to the lowest state of the third rotational band, respectively.

bipartite systems we arrive at the following empirical selection rule.

The matrix elements  $\langle S_{1,a} S_{2,a} S M | H | S_{1,b} S_{2,b} S M \rangle$  of the full Hamiltonian between rotational-band states are (several) orders of magnitude bigger than all other matrix elements if

$$|S_{1,a} - S_{2,a}| - |S_{1,b} - S_{2,b}| = 0. \quad (24)$$

Here  $S_{1,a}$  and  $S_{2,a}$  denote the total spins of sublattices one and two in  $\langle S_{1,a} S_{2,a} S M |$ , respectively. Matrix elements that are not compatible with this rule can be neglected which (after a proper rearrangement) results in a new block-diagonal structure of the reduced Hamilton matrix. These blocks are of smaller size and can be diagonalized separately.

### C. Application to $\{\text{Fe}_{12}\}$

We now apply the approximate diagonalization to an existing molecular spin ring<sup>42</sup> that contains 12  $\text{Fe}^{3+}$  ions with  $s=5/2$ . The system can be modeled by an isotropic Heisenberg Hamiltonian with antiferromagnetic nearest-neighbor coupling  $J$ .<sup>42,43</sup> It was theoretically investigated in Ref. 23 with the help of QMC methods; the exchange parameter was determined to be  $J=-35.2$  K.

Our intention is to show that it is advantageous to combine a stochastic method such as QMC and an exact or approximate diagonalization. In such a combination the role of QMC would be to determine the exchange parameters from thermodynamical observables as done in Ref. 23. For large systems this is practically impossible using exact or approximate diagonalization since diagonalization requires an enormous numerical effort whereas QMC methods scale much more favorable with system size for bipartite systems or even frustrated systems above a certain temperature. The role of exact or approximate diagonalization then would be to use the exchange parameters obtained by QMC for the evaluation of the energy spectrum which then can be used, e.g., to interpret INS measurements.<sup>2,44</sup>

Figure 10 shows the low-energy part of the approximate spectrum of the  $\{\text{Fe}_{12}\}$  compound modeled by an isotropic Heisenberg Hamiltonian. For the approximate calculation of the spectrum full rotational symmetry as well as  $D_2$  point-group symmetry are used. The calculations are performed using eight occupied rotational bands in the  $S=0$  subspace and the corresponding number of bands in subspaces with  $S>0$ . Overall 21 570 976 states have been taken into account, which are only about 15% of all basis states [ $\dim(\mathcal{H})=144,840,476$ ]. Additionally the approximate selection rule given in Eq. (24) was used in order to reduce the dimensionality of the matrices which have to be diagonalized.

Figure 10 also displays the magnetization curve, which is derived from the partition function made of only the approximate energy levels. As one can see the experimental magnetization steps<sup>43</sup> can be reproduced using the approximate diagonalization. We would like to mention that this magnetization curve can be obtained by QMC as well since the system is bipartite.

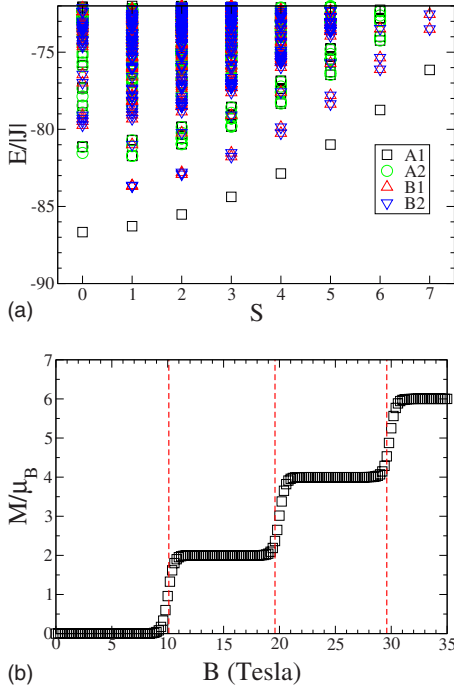


FIG. 10. (Color online) The approximate spectrum of a spin ring with  $N=12$  spins  $s=5/2$  calculated using eight bands, the  $D_2$  point-group symmetry, and the approximate selection rule in Eq. (24) (top). Corresponding magnetization of the system (bottom). The dashed red lines refer to experimental data of the first three magnetization steps from Ref. 43 with  $J=-35.2$  K and  $k_B T/|J|=0.01$ .

#### D. Next-nearest-neighbor coupling—introducing frustration

In the previous parts we demonstrate that the approximate diagonalization scheme based on the rotational-band Hamiltonian yields good results for bipartite, i.e., unfrustrated antiferromagnetic spin systems. We now want to investigate how robust the approximate diagonalization is against the introduction of frustration. To this end we study a spin ring with  $N=8$  and  $s=5/2$  with antiferromagnetic nearest-neighbor coupling  $J=J_{nn}$  and an additional antiferromagnetic next-nearest-neighbor coupling  $J_{nnn}$  which acts frustrating. In a corresponding classical system the Néel state (up-down-up-down-...) would no longer be the ground state, instead canted can occur. One can qualitatively say that with increasing  $J_{nnn}/J_{nn}$  also the frustration increases.

Figure 11 displays the effect of  $J_{nnn}$  in the subspace  $\mathcal{H}(S=0, M=S)$  for the same system that is discussed in Fig. 7 for  $J_{nnn}=0$ . The energy gap between the ground state and the first excited state decreases with increasing frustration. Moreover, the convergence of the ground state as well as of excited states becomes slower. With  $J_{nnn}/J_{nn}=0.4$  the convergence is rather poor and the quantum mechanical ground state now belongs to the irreducible representation  $B_1$  of the symmetry group  $D_8$ . This means that the true ground state is not the result of an adiabatic continuation [ $\lambda:0 \rightarrow 1$  in Eq. (11)] from the ground state of the rotational-band model, which belongs to  $A_1$ . We would just like to mention for the interested reader that this change in the character of the ground state constitutes a so-called quantum phase transition—in this case, for the antiferromagnetic chain with next-nearest-neighbor exchange.

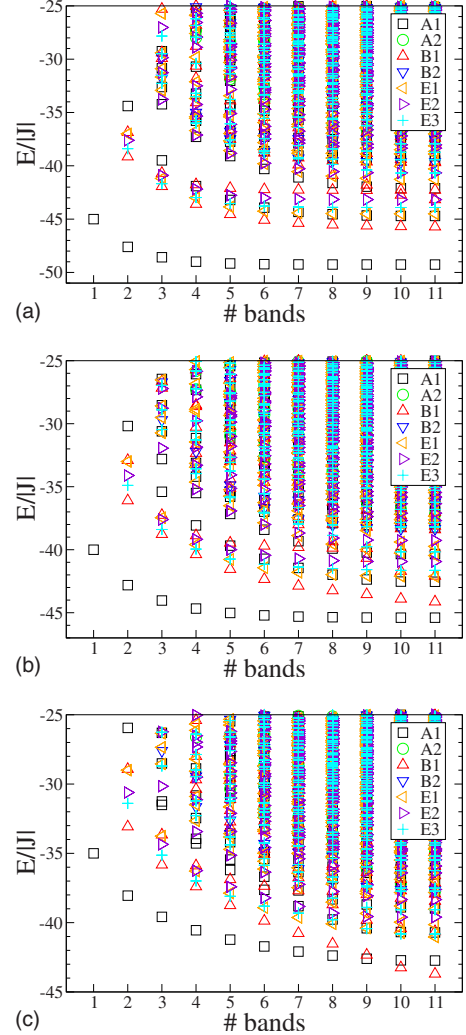


FIG. 11. (Color online) Energy levels of an antiferromagnetic spin ring  $N=8$  with  $s=5/2$  and additional next-nearest-neighbor coupling  $J_{nnn}$  as a function of the number of occupied rotational bands used for diagonalization in subspaces  $S=0$  with  $J_{nnn}/J_{nn}=0.2$  (top),  $J_{nnn}/J_{nn}=0.3$  (center), and  $J_{nnn}/J_{nn}=0.4$  (bottom). The states are labeled according to irreducible representations of  $D_8$ .

Summarizing, if frustration is only small the approximate diagonalization still yields good results. Moreover, approximate selection rule (24) is also applicable which is very helpful in calculating the full spectrum of the system.

## VI. SUMMARY

In this work we have demonstrated that the full spin-rotational symmetry can be combined with arbitrary point-group symmetries. This enables us to obtain exactly the complete energy spectrum of Heisenberg spin systems for so far unprecedented system sizes. Moreover, we have outlined a scheme to approximately diagonalize the Hamilton matrix again using the full spin-rotational symmetry and point-group symmetries. This approximation works well for bipartite antiferromagnetic spin systems. For frustrated systems the quality reduces with increasing frustration. How such a

scheme can be refined for frustrated systems will be the subject of future investigations.

#### ACKNOWLEDGMENTS

Computing time at the Leibniz Computing Center in Garching is gratefully acknowledged as well as helpful ad-

vices of Dieter an Mey and Christian Terboven of High Performance Computing Center, RWTH Aachen in setting up openMP directives. We also thank Boris Tsukerblat for fruitful discussions about the irreducible tensor operator technique and Nedko Ivanov for drawing our attention to some literature. This work was supported within a Ph.D. program of the State of Lower Saxony in Osnabrück.

\*rschnall@uos.de

†jschnack@physik.uni-bielefeld.de

- <sup>1</sup>D. Gatteschi and L. Pardi, *Gazz. Chim. Ital.* **123**, 231 (1993).
- <sup>2</sup>J. J. Borrás-Almenar, J. M. Clemente-Juan, E. Coronado, and B. S. Tsukerblat, *Inorg. Chem.* **38**, 6081 (1999).
- <sup>3</sup>A. Bencini and D. Gatteschi, *Electron Paramagnetic Resonance of Exchange Coupled Systems* (Springer, Berlin, Heidelberg, 1990).
- <sup>4</sup>B. S. Tsukerblat, *Group Theory in Chemistry and Spectroscopy: A Simple Guide to Advanced Usage*, 2nd ed. (Dover, New York, 2006).
- <sup>5</sup>B. S. Tsukerblat, *Inorg. Chim. Acta* **361**, 3746 (2008).
- <sup>6</sup>A. S. Boyarchenkov, I. G. Bostrem, and A. S. Ovchinnikov, *Phys. Rev. B* **76**, 224410 (2007).
- <sup>7</sup>I. Rousochatzakis, A. M. Läuchli, and F. Mila, *Phys. Rev. B* **77**, 094420 (2008).
- <sup>8</sup>C. Raghu, I. Rudra, D. Sen, and S. Ramasesha, *Phys. Rev. B* **64**, 064419 (2001).
- <sup>9</sup>C. Raghu, I. Rudra, D. Sen, and S. Ramasesha, *Phys. Rev. B* **68**, 029902(E) (2003).
- <sup>10</sup>I. Rudra, S. Ramasesha, and D. Sen, *Phys. Rev. B* **64**, 014408 (2001).
- <sup>11</sup>O. Waldmann, *Phys. Rev. B* **61**, 6138 (2000).
- <sup>12</sup>C. Delfs, D. Gatteschi, L. Pardi, R. Sessoli, K. Wieghardt, and D. Hanke, *Inorg. Chem.* **32**, 3099 (1993), ([pubs.acs.org/doi/pdf/10.1021/ic00066a022](https://pubs.acs.org/doi/pdf/10.1021/ic00066a022) and [pubs.acs.org/doi/abs/10.1021/ic00066a022](https://pubs.acs.org/doi/abs/10.1021/ic00066a022)).
- <sup>13</sup>I. G. Bostrem, A. S. Ovchinnikov, and V. E. Sinitsyn, *Theor. Math. Phys.* **149**, 1527 (2006).
- <sup>14</sup>V. E. Sinitsyn, I. G. Bostrem, and A. S. Ovchinnikov, *J. Phys. A: Math. Theor.* **40**, 645 (2007).
- <sup>15</sup>V. Fack, S. N. Pitre, and J. van der Jeugt, *Comput. Phys. Commun.* **101**, 155 (1997).
- <sup>16</sup>V. Fack, S. N. Pitre, and J. van der Jeugt, *Comput. Phys. Commun.* **86**, 105 (1995).
- <sup>17</sup>S. R. White, *Phys. Rev. B* **48**, 10345 (1993).
- <sup>18</sup>M. Exler and J. Schnack, *Phys. Rev. B* **67**, 094440 (2003).
- <sup>19</sup>U. Schollwöck, *Rev. Mod. Phys.* **77**, 259 (2005).
- <sup>20</sup>C. Lanczos, *J. Res. Natl. Bur. Stand.* **45**, 255 (1950).
- <sup>21</sup>A. W. Sandvik and J. Kurkijärvi, *Phys. Rev. B* **43**, 5950 (1991).
- <sup>22</sup>A. W. Sandvik, *Phys. Rev. B* **59**, R14157 (1999).
- <sup>23</sup>L. Engelhardt and M. Luban, *Phys. Rev. B* **73**, 054430 (2006).
- <sup>24</sup>K. Bärwinkel, H.-J. Schmidt, and J. Schnack, *J. Magn. Magn. Mater.* **212**, 240 (2000).
- <sup>25</sup>D. A. Varshalovich, A. N. Moskalev, and V. K. Khersonskii, *Quantum Theory of Angular Momentum* (World Scientific, Singapore, 1988).
- <sup>26</sup>G. S. Griffith, *On the General Theory of Magnetic Susceptibilities of Polynuclear Transition-metal Compounds*, Structure and Bonding Vol. 10 (Springer, Berlin, Heidelberg, 1972), p. 87.
- <sup>27</sup>B. S. Tsukerblat, M. I. Belinskii, and V. E. Fainzil'berg, *Sov. Sci. Rev.* **9**, 337 (1987).
- <sup>28</sup>M. Tinkham, *Group Theory and Quantum Mechanics* (Dover, New York, 2003).
- <sup>29</sup>E. Weisstein, Mathworld, <http://mathworld.wolfram.com>
- <sup>30</sup>A. J. Blake, R. O. Gould, C. M. Grant, P. E. Y. Milne, S. Parsons, and R. E. P. Winpenny, *J. Chem. Soc. Dalton Trans.* **1997**, 485.
- <sup>31</sup>C. P. Pradeep, D.-L. Long, P. Kögerler, and L. Cronin, *Chem. Commun. (Cambridge)* **2007**, 4254.
- <sup>32</sup>R. Schmidt, J. Schnack, and J. Richter, *J. Magn. Magn. Mater.* **295**, 164 (2005).
- <sup>33</sup>J. Schnack, R. Schmidt, and J. Richter, *Phys. Rev. B* **76**, 054413 (2007).
- <sup>34</sup>J. Schnack and R. Schnalle, *Polyhedron* (to be published).
- <sup>35</sup>D. Coffey and S. A. Trugman, *Phys. Rev. B* **46**, 12717 (1992).
- <sup>36</sup>O. Waldmann, *Phys. Rev. B* **75**, 012415 (2007).
- <sup>37</sup>J. Schnack and M. Luban, *Phys. Rev. B* **63**, 014418 (2000).
- <sup>38</sup>O. Waldmann, *Phys. Rev. B* **65**, 024424 (2001).
- <sup>39</sup>J. Schnack, M. Luban, and R. Modler, *Europhys. Lett.* **56**, 863 (2001).
- <sup>40</sup>A. Lascialfari, D. Gatteschi, F. Borsa, and A. Cornia, *Phys. Rev. B* **55**, 14341 (1997).
- <sup>41</sup>A. Lascialfari, D. Gatteschi, F. Borsa, and A. Cornia, *Phys. Rev. B* **56**, 8434 (1997).
- <sup>42</sup>A. Caneschi, A. Cornia, A. C. Fabretti, and D. Gatteschi, *Angew. Chem., Int. Ed.* **38**, 1295 (1999).
- <sup>43</sup>Y. Inagaki, T. Asano, Y. Ajiro, Y. Narumi, K. Kindo, A. Cornia, and D. Gatteschi, *J. Phys. Soc. Jpn.* **72**, 1178 (2003).
- <sup>44</sup>R. Basler, C. Boskovic, G. Chaboussant, H. U. Güdel, M. Murrie, S. T. Ochsenbein, and A. Sieber, *ChemPhysChem* **4**, 910 (2003).